J Fluoresc (2007) 17:350–360
DOI 10.1007/s10895-007-0192-2

ORIGINAL PAPER

Visualization of Arginine Influx into Plant Cells Using a Specific FRET-sensor

Martin Bogner · Uwe Ludewig

Received: 9 January 2007 / Accepted: 3 April 2007 / Published online: 10 May 2007

Abstract Amino acids are not only the building blocks of proteins, but are the metabolic precursors of a variety of primary and secondary metabolites. In order to detect and visualize how plants transport, sense, and store amino acids with sub-cellular specificity, chimeric fluorescent proteins that respond to changes in amino acid concentrations were constructed. The reporter element of these sensors consists of a periplasmic bacterial protein that undergoes large, non-enzymatic conformational changes upon binding of its substrate. The receptor protein was attached to ECFP and an environmentally insensitive YFP derivative at opposite ends. Fluorescence resonance energy transfer changes were specifically observed after addition of arginine and to a lesser extent ornithine. The recombinant sensor showed a concentration-dependent increase in the fluorescence ratio with an apparent in vitro affinity for arginine of ~2 mM. A mutation in the binding pocket lowered the affinity and decreased the specificity. When expressed in *E. coli*, an increase in the fluorescence ratio was specifically detected after exposure to arginine and ornithine. Transient expression of the sensor in plant cell protoplasts and stable expression in Arabidopsis roots revealed specific fluorescence changes upon addition of arginine. The analysis suggests that fluorescent amino acid sensors may be versatile tools for studying the in vivo dynamics of metabolism and compartmentalization in plants.

M. Bogner · U. Ludewig (✉)
Zentrum für Molekularbiologie der Pflanzen (ZMBP),
Pflanzenphysiologie, Universität Tübingen,
Auf der Morgenstelle 1, 72076 Tübingen, Germany
e-mail: uwe.ludewig@zmbp.uni-tuebingen.de

Keywords Metabolite imaging · FRET-imaging · Periplasmic binding protein · Arabidopsis · Amino acid sensor · Arginine metabolism

Introduction

Amino acids are the building constituents of proteins and the metabolic precursors of nucleic acids. They are required for the synthesis of many primary and secondary metabolites. The amino acid composition of plant tissues varies significantly during the night and light period of a single day. In addition to their nutritional role, some amino acids have been suggested to have a signaling function [1]. For example, exogenously applied glutamate affects root morphology [2].

The amino acid composition greatly depends on nutrient supply and environmental conditions. Besides that, a number of feedback-regulators appear to optimize the composition for protein synthesis during all developmental stages [3]. Several amino acids, such as proline, play further roles e.g. they act as compatible solutes under drought conditions. Arginine (Arg), frequently a major amino acid translocated in the xylem, has often been assigned a nitrogen storage function and generally reports nitrogen sufficiency. Arg is the major storage and nitrogen reserve amino acid in germinating soybean [4].

Amino acids and other metabolites have been simultaneously measured with enormous sensitivity by a number of different techniques, including those based on fractionation and non-aqueous density gradient centrifugation, but these methods report a static metabolite distribution [5]. The large-scale parallel analysis of many metabolites provides unprecedented knowledge about the metabolic constituents of the plant, but most approaches have limitations due to poor cellular or sub-cellular resolution [6]. More recently,

several fluorescent biosensors have been developed and introduced to specifically monitor sugars, amino acids or nutrients within fluids or cells [7, 8]. Only recently, the expression of a sugar biosensor and the monitoring of sugar levels has been reported in plants [9]. Fluorescent metabolite sensors appear to be especially promising for non-invasive imaging of the cellular and sub-cellular metabolites in cells that are experimentally less accessible, although this method does have other limitations [8].

Cellular imaging, e.g. with calcium-specific fluorescent probes, has been used as an elegant tool to uncover the surprising complexity of cytosolic calcium dynamics in animal, yeast and plant cells. Such sensors detected oscillations that are of functional significance in guard cell regulation [10]. The fluorescent sensors for calcium, commonly known as cameleon, contain a reporter-domain consisting of calmodulin and the M13 domain, fused with spectral variants of the green fluorescent protein [11]. Based on this principal design, a wide variety of reporters for other cellular and biochemical events, including indicators for cGMP, sugars and reporters for the activities of protein kinases, have been developed [11, 12]. The common reporter element in such sensors is a sterically separated donor-acceptor Förster resonance energy transfer (FRET) pair, which in most cases includes the enhanced cyan fluorescent protein (ECFP) and an improved, environmentally insensitive, version of the yellow fluorescence protein (YFP). By using the same principal design, a glutamate sensor was developed using the bacterial glutamate-binding protein ybeJ from *E. coli* as a recognition element [13].

Periplasmic binding proteins belong to a large group of structurally similar proteins that recognize a different metabolite or ion. These proteins have been recognized as potential specific metabolite and nutrient sensors. A variety of biosensors was constructed by covalent linkage of a fluorescent chromophore to such proteins [14]. However, the necessity to covalently couple small fluorophore dyes to the binding proteins reduces the usability of such biosensors for cellular and sub-cellular metabolite sensing.

The bacterial glutamine binding protein (QBP) from *E. coli* is involved in glutamine acquisition in that organism and undergoes reversible conformational changes upon binding of the ligand. QBP mutants with sulfhydryl-reactive fluorescent probes covalently attached to engineered cysteins showed the potential of QBP as a glutamine biosensor with an apparent affinity of 160 nM [15]. The purified QBP protein had been shown to have high specificity [16]. Of the naturally occurring amino acids, only glutamine bound with high affinity in the μM range [16]. The QBP protein has been crystallized in two conformations: in an open form, without glutamine (PBD accession code: 1GGG) [17] and in a closed form, in association with glutamine (PBD accession code: 1WDN) [18]. The substrate-binding pocket is located in the center of the protein and is embedded between two lobes that apparently move by a hinge-like motion with a slight rotation [18].

In this study, genetically encoded ratiometric fluorescent amino acid sensors were constructed, purified, characterized and used in bacteria as well as in plants. These sensors are based on the bacterial periplasmic protein QBP as a reporter element, which is coupled to two spectral GFP variants. Initial modeling suggested that the movement of the attached chromophores that resulted from substrate binding is maximal with the insertion of one chromophore into a lobe of QBP that is positioned opposite to its carboxy-terminus. The second chromophore was attached to the carboxy-terminus. This chimeric sensor specifically responded to Arg and ornithine (Orn) with FRET ratio changes, and it reported the uptake of these amino acids into bacteria that expressed the sensor. In addition, these sensors have been used in plants to specifically detect and visualize Arg influx into the cytoplasm. The results suggest that genetically encoded recombinant fluorescent sensors will be versatile tools for dissecting the amino acid metabolism and compartmentation in plant cells.

Experimental

Construction, expression and purification of fluorescent sensors

A cassette was constructed as a translational fusion of citrine, a mutant version of the enhanced yellow fluorescent protein (EYFP, Clontech) via a linker to the enhanced cyan fluorescent protein (ECFP) (Clontech). The citrine sequence was constructed by replacing the codon for Gln at position 69 by methionine in EYFP (Clontech) using the QuickChange method from Stratagene. The citrine sequence was shortened by six codons at the 5′ end and ten codons at the 3′ end. The ECFP sequence was shortened by four codons at the amino-terminus. This cassette had *BamHI* and *XbaI* sites in front of the shortened citrine sequence and the linker between citrine and ECFP contained *SpeI* and *AscI* sites, respectively. The shortened ECFP sequence was followed by an *AvrII* restriction site, a STOP codon, and a *SalI* restriction site.

The gene encoding the periplasmic QBP was amplified from genomic *E. coli* DNA by PCR. The amino-terminal fragment (coding for amino acids Ala1-Asn98) lacked the coding sequence for the first 22 amino acids (the signal peptide). The forward primer sequence was: 5′-GAGA GGATCCATGGCGGATAAAAAATTAGTTGTCG-3′ and contained a *BamHI* site. The reverse primer with *XbaI* site

was: 5′-GAGTCTAGACCATTGTTAGCTTTCACCAT CAC-3′. The primers for the carboxy-terminal fragment were: 5′-GAGACTAGTGCAGTAGGCAACGATGT GAAAAGCG-3′ and 5′-GAGGCGCGCCCTTTCGGTT CAGTACCGAACCATTT-3′. These primers included *SpeI* and *AscI sites.* Insertion of these fragments into the citrine/ECFP cassette using appropriate restriction enzymes yielded the QBP/cirine/ECFP sensor construct. A schematic drawing of the construct is given in Fig. 1b. The mutations threonine at position 70 replaced by alanine (T70A) and aspartate to asparagine (D157N) in QBP were generated by using the QuikChange method (Stratagene).

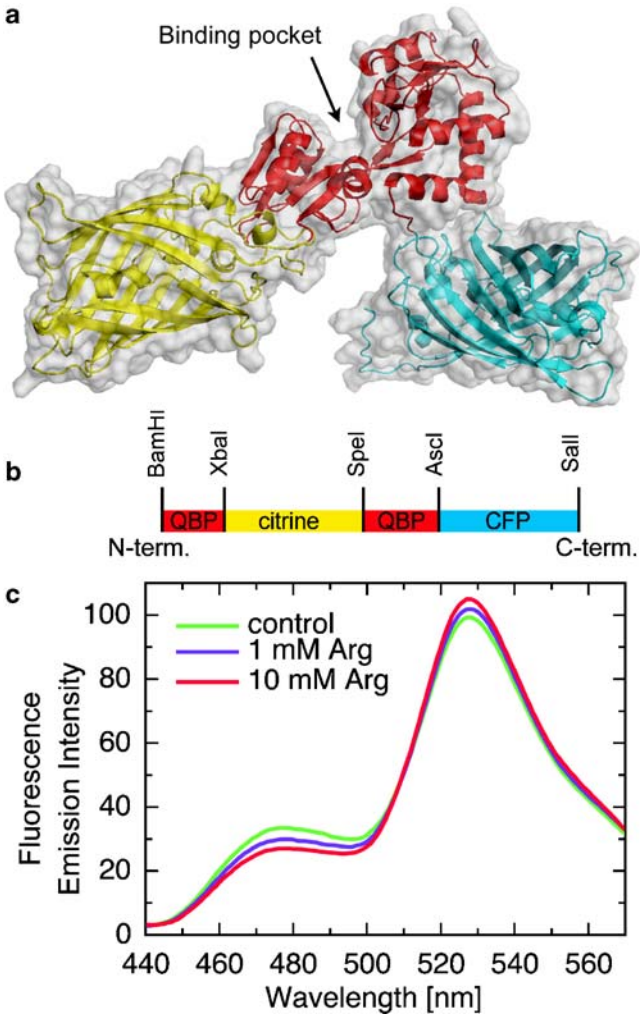

Fig. 1 Design of the amino acid FRET-sensor. **a** Modeled structure of a chimeric protein composed of citrine (*yellow*), the open conformation of QBP (*red*) and ECFP (*cyan*). **b** Linear representation of the sequence of the same construct as in **a**. The QBP sequence was split into two parts and the citrine sequence was inserted in frame using minimal linkers. **c** Changes in the emission spectrum of the construct upon excitation with blue light (433 nm) and addition of Arg (1 and 10 mM)

In the resultant chimeric proteins, the core sequence of citrine was inserted between position Asn98 and Asn99 in QBP. The resulting protein linker sequences are explicitly given: (amino-terminal part of QBP) …VKANNGLDEEL… (core sequence of citrine)…AAGTSAVGNDVKSVK (carboxy- terminal part of QBP)… KWFGTEPKGRAGEELF… (core sequence of ECFP). The amino acid numbers are given according to the processed QBP protein without signal peptide, starting with Ala at position 1. All constructs were verified by full-length sequencing.

The chimeric fragment was inserted into pET41 (Novagen) using *BamHI* and *SalI*. This adds an *in frame* His-tag at the amino-terminus of the sequence. Constructs were transferred into *E. coli* BL21(DE3)Gold (Stratagene) using heat shock. Cells were grown for 24 h at 20°C to an OD of 0.6–0.8, induced with 0.2 mM IPTG and grown for 2 days at 20°C in the dark. Cells were harvested by centrifugation, resuspended in 20 mM Tris·Cl, pH 8.0, and disrupted by ultrasonication. Recombinant proteins were purified by His-Bind affinity chromatography resin (Novagen). Binding to the resin was performed at 4°C for 2 h and then washed with 20 mM Tris·HCl. The columns were incubated overnight on ice and subsequently washed with 20 mM Tris·HCl containing 20 mM imidazole at pH 8.0, and eluted with 200 mM imidazole in Tris·HCl, pH 8.0.

In vitro characterization of the sensors

Emission spectra and ligand binding curves were obtained from purified protein after overnight storage at 4°C. Emission spectra were recorded spectrofluorometrically (SFM25, Kontron, Zürich) from purified proteins in 20 mM Tris·HCl buffer (which contained a final concentration of 20 mM imidazole, pH 8.0) after excitation of ECFP at 433 nm with horizontal analyzer and polarizer positions. The excitation bandwidth was 10 nm and emission bandwidth 20 nm.

A monochromator microplate reader (Safire) was used to determine substrate binding affinities. Purified proteins were diluted in 20 mM Tris·HCl buffer (pH 8.0, final concentration of 11 mM imidazole). The excitation filter was 433/12 nm; emission filters for ECFP and Citrine were 475/12 and 528/12 nm, respectively. The apparent K_d of each construct to different ligands was determined by fitting the data with a simple binding isotherm: $I=(r-r_{min})/(r_{max}-r_{min})=[L]/(K_d+[L])$, where [L] is the ligand concentration, r the ratio, r_{min} the minimum ratio in the absence of ligand and r_{max} the maximum ratio with saturating ligand. A Hill coefficient of $n=1$ was determined in all measurements with the equation $S=(n[L]_n)/(K_d+[L]_n)$. Measurements were performed with at least three independent protein extracts. The fluorescence resonance energy transfer (FRET) ratio

was determined as the fluorescence intensity at 528 nm divided by the intensity at 475 nm.

In vivo characterization of the sensors

The monochromator microplate reader (Safire) was used to measure ratio changes from *E. coli* cell suspensions expressing the sensors. Cells were harvested, adjusted to OD 3.0–3.5 and kept in 20 mM Tris-buffered solution at pH 8.0 and were starved of nitrogen for 1 h. The excitation filter was 433/12 nm; emission filters for ECFP and Citrine were 475/12 and 528/12 nm, respectively.

Live cell imaging

Protoplast and plant imaging was performed on a fluorescence microscope (DMIRB, Leica) with a cooled charge-coupled device camera (Sensys Photometrics, Tucson, AZ) and 40× objective. Dual emission intensity ratio was recorded by using METAFLUOR 4.5 software (Universal Imaging, Media, PA) with 436/20 excitation, two emission filters (480/40 for ECFP and 535/30 for EYFP) and a neutral density filter (1 or 5% transmission) on the excitation port. Methanol washed cover slides were used to fix the protoplasts. Amino acids were slowly added to the bath solution using a nanoliter pipette positioned closely to the protoplast in focus.

Confocal images were taken on a Leica DMRE microscope equipped with a confocal head TCS SP (Leica, Wetzlar, Germany) and a 63× water immersion objective. The FRET sensitized emission tool without background subtraction of the Leica confocal software was used to record and display the data. The data were processed and displayed with METAFLUOR 4.5 software and Adobe Photoshop. Plants were positioned on self-built perfusion chambers (~80 µl volume) that were based on cover slides. To fix the plants, the slides were coated with a thin layer of viscous superglue, plants were carefully positioned, rinsed with a large volume of the growth medium and covered with a cover slip. The complete exchange of the external growth medium by the same medium with Arg was completed within a few seconds. Images were taken from 6–10 day old plants.

Plant expression, transformation and growth

The sensor sequences were shuttled into the plant expression vector *pPTbar*, a derivative of the *pPZP212* vector [19] containing the BASTA resistance, a *35S*-promoter and a *rbcs*-terminator. The restriction enzymes used were *BamHI* and *SalI*. *A. thaliana* plants (ecotype *Col-0*) were grown in soil and transformed using the GV3101 agrobacterium strain by spraying. Seeds were germinated in the dark for 4 days on agar plates (0.8%) containing minimal nutrient medium with 100 µM NH_4NO_3 as nitrogen source. Selection for transgenic plants was performed with the addition of 4 µM N-Methyl sulfoximine (MSX) to the agar plates. Only plants from the T1 generation were used for Arg imaging, although fluorescence was frequently also observed in subsequent generations.

Dark grown suspension cultures were used for the preparation of protoplasts, which were isolated and transiently transfected via a PEG-based method at the transformation unit of the ZMBP (http://www.uni-tuebingen.de/ZMBP/centfac/transf/index.html).

Amino acid content

Plants were grown on Murashige-Skoog (MS) medium (Duchefa, Netherlands) with 0.8% agar for 14 days at 22°C with 16 h light. To obtain sufficient amount of plant material the stably expressing QBP/citrine/ECFP plants of the T2 generation were taken. Wild type and sensor expressing plants were ground in liquid N_2 and amino acids were extracted by adding 80 and 20% methanol. Both extracts were pooled and dried under vacuum. The pellet was resuspended in lithium buffer (0.7% lithium acetate, 0.6% LiCl; Pickering Laboratories, Mountain View, CA) containing 0.2 mM norleucine as an internal standard. Amino acids were separated by HPLC on a cation–exchange column (high efficiency fluid column, 3 mm×150 m; Pickering Laboratories) using lithium buffer as eluant. The amino acids were dramatized with ninhydrine before photometric detection.

Molecular modelling

Molecular modeling was essentially performed as described [20]. Briefly, the primary sequence of QBP/citrine/ECFP was structurally fitted using MODELLER 7v7 (available at http://salilab.org/modeller/) based on the available structures of QBP and GFP. The structures were evaluated using the WHATIF program (http://biotech.ebi.ac.uk:8400/) and Procheck (http://www.biochem.ucl.ac.uk/~roman/procheck/procheck.html). Energy minimization of the model was performed for 10 psec using NAMD2.5 (http://www.ks.uiuc.edu/Research/namd/), using the Amber7 force field.

Results

Development of a fluorescent sensor for in vivo imaging of amino acid levels

The glutamine binding protein (QBP) from *E. coli* is an excellent candidate for the development of fluorescent amino acid sensors, as it exclusively binds glutamine with

high affinity and exhibits a large conformational movement between the two globular domains upon ligand binding [18].

QBP was fused to citrine (a YFP variant with reduced environmental sensitivity [21]) and ECFP, a widely used donor/acceptor FRET pair. A comparison of the open and ligand-bound closed forms of QBP showed that the conformational differences between the amino- and carboxy-tail of QBP were rather small. Since the fluorescent readout and FRET in such constructs depend on the distance change between the chromophores, attaching the GFP variants at the amino and carboxy-terminus of QBP was not expected to produce large substrate-dependent FRET ratio changes. Such sensors, however, have been constructed and give small ratio changes with the addition of substrate [13]. The largest distance changes within QBP are apparently not between the amino- and carboxy-terminus, but between other parts of the QBP protein. To restrict the positions and dipole orientations of both chromophores, the linkers between all protein parts were minimized (as detailed in methods) and ECFP was invariably attached to the carboxy-terminus.

Molecular modeling was used to identify an optimal sensor construct. A molecular minimization procedure was applied to all models to reduce amino acid clashes and unrealistic constraints in the computer simulations. The computer models suggested that the insertion of citrine into a loop positioned in the globular domain opposite the carboxy-terminus (at position Asn 98) might result in an optimal construct. Such an insertion, however, partially distorted the protein fold in the vicinity of the ligand binding pocket. This region is in close proximity to the amino acid side chain of the bound ligand. As a result, the substrate specificity of the QBP protein with an inserted YFP chromophore into one lobe was likely to be somewhat altered compared with that of the original QBP. A picture of the model of an optimal construct is shown in Fig. 1a. In this construct, the sequence of QBP was divided into two parts and citrine was inserted between positions 98/99. A linear diagram showing the arrangement of the sensor cassette with the used restriction sites is shown in Fig. 1b. The chimeric protein was purified and the emission spectra changed after the addition of the amino acid Arg (Fig. 1c).

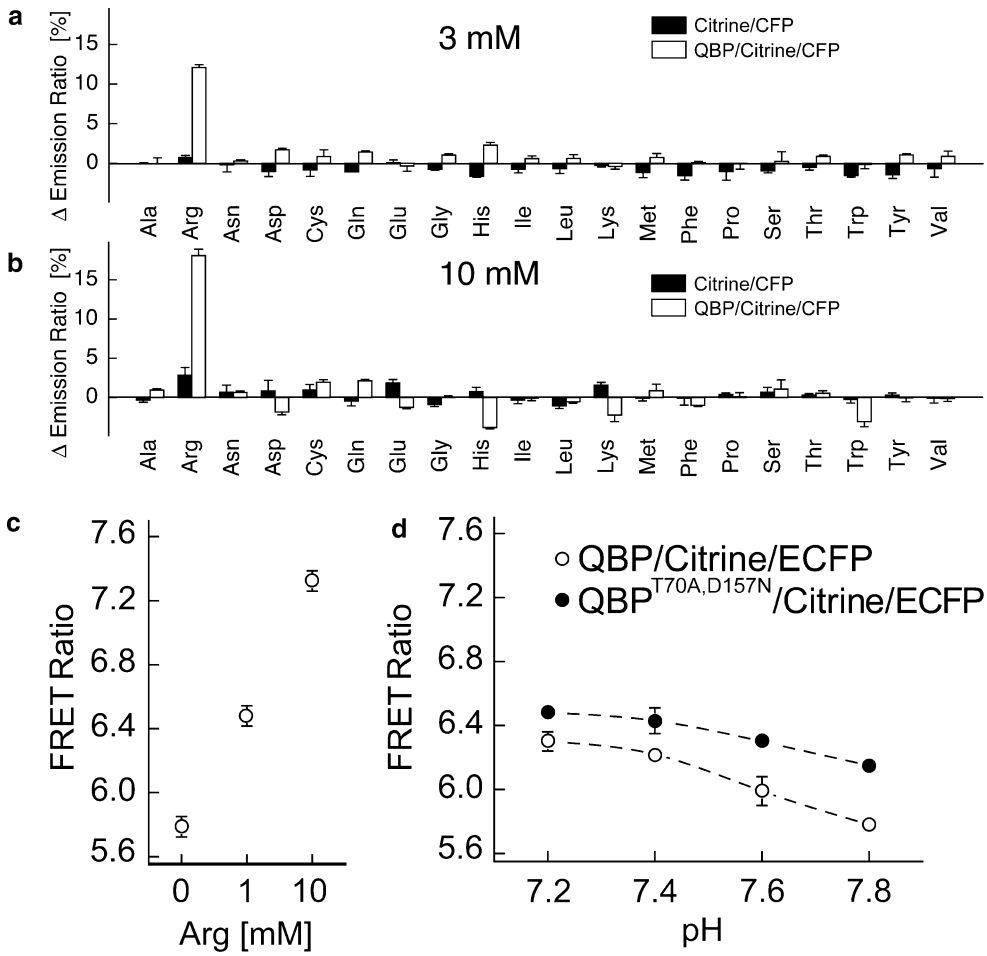

Fig. 2 Specificity of the FRET sensor to Arg. Relative fluorescence changes upon addition of all natural proteinogenic amino acids at 3 mM **a** and 10 mM **b** to the QBP/Citrine/ECFP chimera and a construct without glutamine binding protein, consisting of only citrine fused to ECFP. **c** FRET ratio in response to Arg **d** pH-dependence of QBP/Citrine/ECFP and a double mutant $QBP^{T70A,D157N}$/Citrine/ECFP in the absence of Arg

In vitro properties of the Arg sensor

The specificity of fluorescence was then determined for all proteinogenic amino acids at a concentration of 3 and 10 mM (Fig. 2). Arg, but not glutamine, affected the fluorescence ratio. As a control, a chimera of citrine and ECFP was used. This protein, without the periplasmic domain, did not change its fluorescence significantly after the addition of any amino acid at 3 or 10 mM, suggesting that the chromophores were little affected by the addition of amino acids (Fig. 2a,b). The fact that the chimeric protein had a different substrate specificity and affinity compared to QBP was not unexpected, based on our molecular modeling. The chimeric QBP/citrine/ECFP sensor was further tested for its environmental sensitivity to pH. The fluorescence of both ECFP and citrine is known to be quenched by acidic pH [22]. In the pH range of the cytoplasm, the fluorescence ratio of the QBP/citrine/ECFP construct slightly decreased with more alkaline pH (Fig. 2d). However, the pH-dependence was rather small compared to the large changes induced by Arg (Fig. 2c) and were similar in another control construct, which had two mutations in the binding pocket of the receptor domain (Fig. 2d; see below).

Mutations within the QBP binding pocket should affect the affinity of substrate binding and/or its specificity. However, mutations that reduce the binding affinity, but retain the specificity of QBP, have not been reported. Interestingly, the binding elements of the glutamine binding protein QBP are closely related to those of the mammalian glutamate receptors in structure and sequence (Fig. 3b). A detailed mutational analysis of the binding pocket of a related mammalian ionotrophic glutamate receptor has been performed [23]. The comparison of the related proteins suggested that several residues might affect the substrate affinity in QBP. The mutation T488A in the binding pocket of a mammalian glutamate receptor reduced the affinity to glutamate by over 500-fold [23]. The corresponding mutation (threonine at position 70 to alanine) was inserted into the chimeric QBP/citrine/ECFP sensor. This threonine is located in the hinge region of QBP and forms a hydrogen bond with the ligand (Fig. 3a). As expected, the mutation altered the specificity of the chimeric protein and allowed glutamine to cause fluorescence changes (Fig. 3c). In addition, the magnitude of FRET ratio changes was affected. The introduction of an additional second mutation, D157N (Fig. 3a), into the mutant sensor completely abolished the sensitivity to Arg (Fig. 3d). In contrast to the insensitivity to Arg, the double mutant construct responded similarly to the pH as the QBP/citrine/ECFP sensor (Fig. 2d). Preliminary analysis showed that addition of other amino acids altered fluorescence in this double mutant construct (*data not shown*).

Detailed analysis identified that Orn, but not citrulline, induced FRET ratio changes in the QBP/citrine/ECFP construct. However, the total ratio changes with Orn were smaller than with Arg (Fig. 4). For the construct containing the wild type sequence of QBP, an apparent K_d=2.0 mM

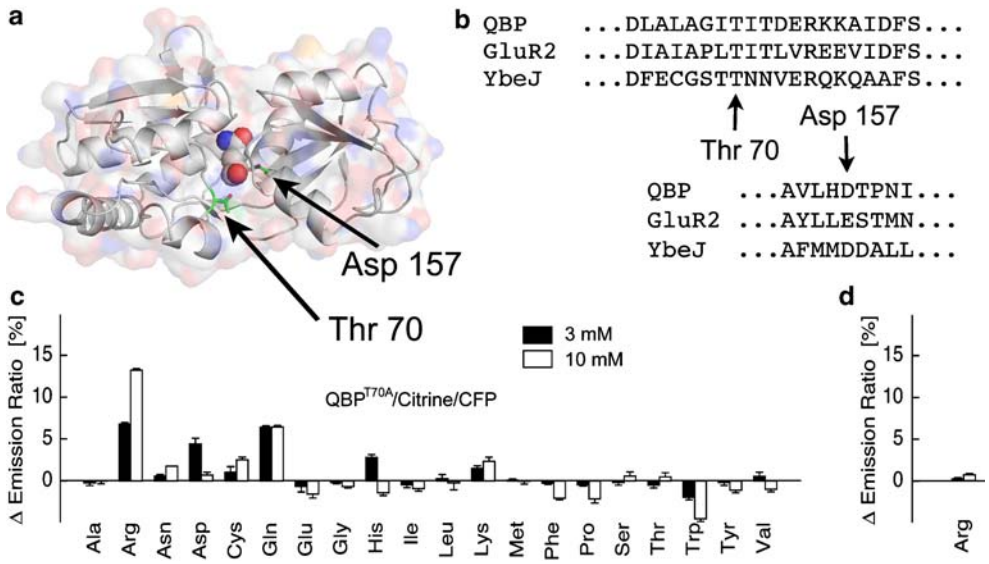

Fig. 3 Alteration of the substrate specificity by mutations in the binding pocket. **a** Position of the mutated sites (threonine 70 and glutamate 157, shown in *green*) in the crystal structure of the closed conformation of QBP (PDBcode: 1WDN). Glutamine in the binding pocket is shown as a spherical molecule and orients with its side chain away from the threonine at position 70. **b** Sequence comparison of QBP, the glutamate/aspartate binding protein YbeJ from *E. coli*, and the binding site of a mammalian glutamate receptor. Positions 70 and 157 are shown by the *arrows*. **c** Fluorescence changes of the mutated QBP^{T70A}/Citrine/ECFP with all proteinogenic amino acids at 3 and 10 mM concentration. **d** Fluorescence ratio changes of the double mutant $QBP^{T70A,D157N}$/Citrine/ECFP with Arg at 3 and 10 mM. concentration

for Orn was determined. This was very similar to the apparent K_d=2.1 mM that was determined for Arg. As noted earlier, the addition of glutamine did not reveal fluorescence changes between 0 and 100 mM (Fig. 4).

The FRET ratio changes in the construct containing the mutation T70A were saturated at an apparent K_d=3.2 mM for Arg and apparent K_d=9.2 mM for Orn. The FRET ratio of the T70A mutant construct also responded to glutamine, but with micromolar affinity. In all determinations, the Hill constant was determined as 1, suggesting a single binding site in all constructs. Binding of substrates to the sensors was reversible, as determined by repeated fluorescence analysis of His-purified proteins after incubation in substrate and subsequent washing (*data not shown*).

In vivo imaging of cytosolic Arg uptake in bacteria

The versatility of the recombinant QBP/citrine/ECFP proteins was tested in vivo, by expression in the cytosol of *E. coli*. Bacterial suspensions of *E. coli* culture had an increasing FRET ratio after the external application of Arg or Orn (Fig. 5a). The FRET ratio of these cells increased for several minutes and saturated after 15 min. This is compatible with the saturable uptake of these amino acids into the bacterial cytoplasm. In *E. coli,* a variety of different low and high affinity systems catalyze efficient uptake of amino acids into the cytoplasm [24]. When several different amino acids were applied, a FRET ratio increase was specifically recorded after the addition of Arg, and to a lesser extent of Orn. In another preparation, the effect of addition of other amino acids was tested. Glu, Asp and Pro did not increase the ratio (Fig. 5b). In contrast, Gln slightly decreased the ratio, which may reflect secondary metabolic effects on the sensor. The results show the overall specificity of the sensor in vivo.

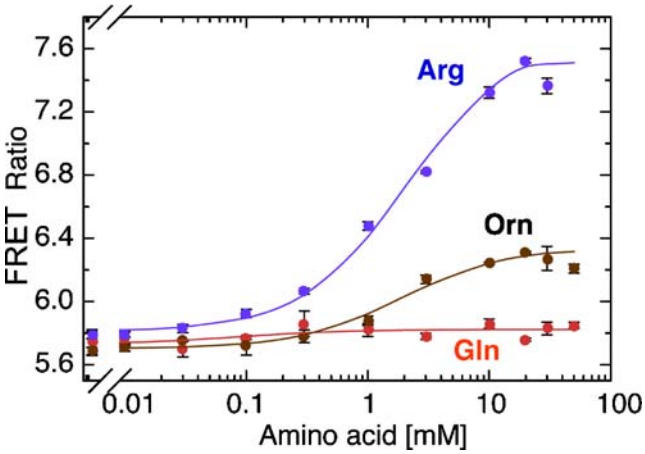

Fig. 4 Concentration dependence of the FRET ratio changes with addition of glutamine (*red*), Arg (*blue*) and Orn (*brown*). Binding isothermes for the sensor containing the wild type sequence of QBP are given as FRET ratio (the fluorescence intensity at 528 nm divided by the intensity at 475 nm)

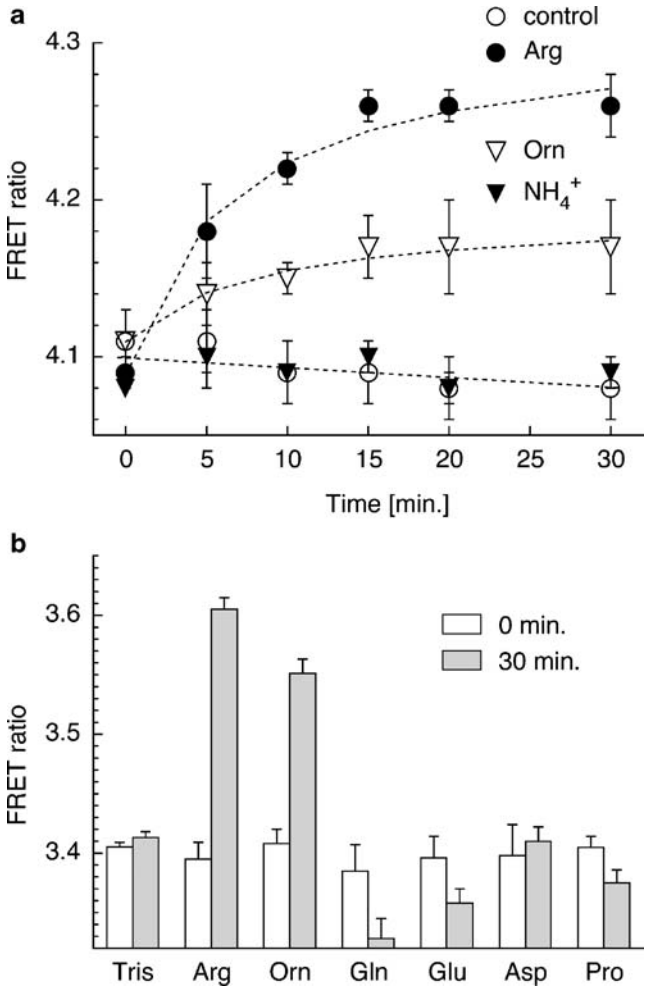

Fig. 5 Fluorescence changes in bacterial cell suspensions expressing the QBP/Citrine/ECFP sensor. **a** Time course of FRET ratios as calculated from the intensities at 528 nm/475 nm after addition of Tris-buffered solution without nitrogen (pH 8.0, *open circles*) and Tris buffer containing 1 mM Arg (*closed circles*), 1 mM Orn (*open triangle*) or 1 mM ammonium (*closed triangle*). **b** FRET ratio of bacterial cells before and after 30 min of incubation with different amino acids at 2 mM. Similar results were obtained using 1 mM of each amino acid

In vivo imaging of cytosolic Arg in plant protoplasts

The sensors were transiently expressed in plant protoplasts from dark grown suspension cultures and studied using an inverted fluorescence microscope. The fluorescence was excluded from the vacuolar lumen (Fig. 6a). Without or with micromolar the addition of Arg, the overall fluorescence and the FRET ratio of the protoplast in focus slowly decreased (*data not shown*). This is compatible with the

well known bleaching of the chromophores and has been reported for the YFP-variant citrine [21]. The addition of millimolar Arg, slowly but consistently, increased the FRET ratio. Due to the relatively large background in plant protoplasts, the FRET ratio increase was strongest in regions with high fluorescence. Examples of the FRET levels in false colors before and after the Arg application to a single protoplast are shown in Fig. 6b,c. As an increase in the FRET ratio of protoplasts was never observed without the addition of Arg, but consistently after addition of high Arg concentrations, the data suggest that the Arg influx is responsible for the FRET ratio increase.

In addition, the total FRET ratio from a different, continuously monitored protoplast is seen in Fig. 6f. The FRET ratio without Arg is shown in Fig. 6d, and after the addition of Arg in Fig. 6e. Slow replacement of the washing solutions flushed away or moved the protoplasts in most

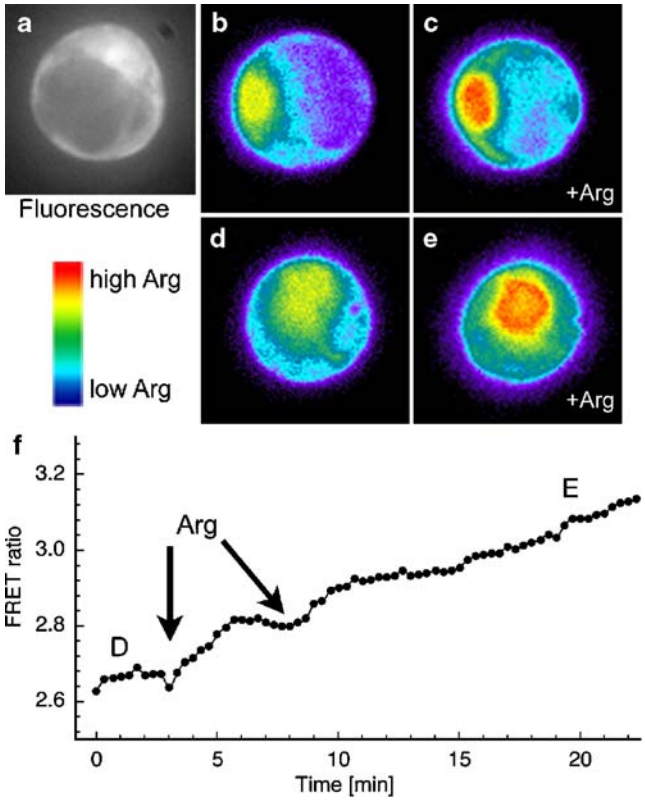

Fig. 6 Fluorescence changes in the plant cytosol upon addition of Arg. **a** Typical fluorescence (at 535 nm) from a protoplast expressing the QBP/Citrine/ECFP sensor. The fluorescence was excluded from the vacuole. **b**,**c** FRET ratios (535/480 nm) of a protoplast before and 5 min. after addition of Arg (2,5 mM final concentration). **d**,**e**,**f** Different protoplast at the beginning **d** of the experiment and 20 min after addition of Arg **e**. **f** Time course of fluorescence of the same protoplast after Arg was carefully added to the medium using a nanoliter pipette to a final concentration of 2,5 mM. The arrows show the timepoints where Arg was added and the letters show the timepoints where ratio snapshots were taken. Similar results were obtained with n=6 protoplasts

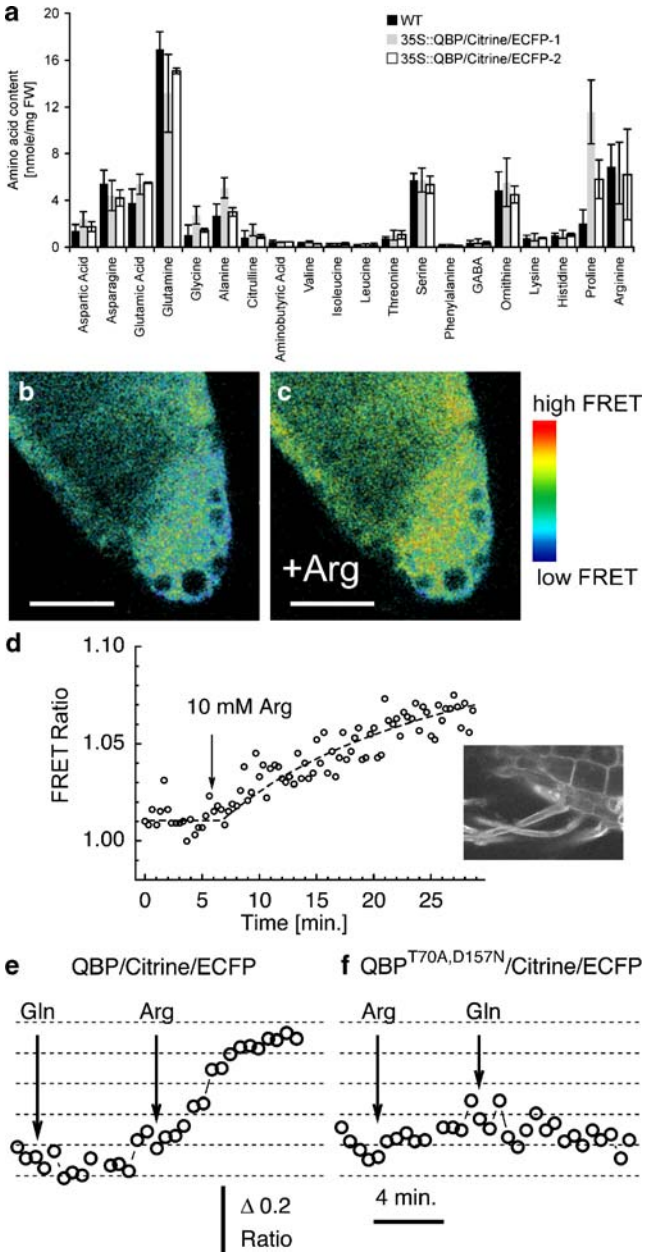

Fig. 7 Arginine specificity of fluorescence changes in plants expressing the QBP/Citrine/ECFP sensor. **a** Amino acid content in 14d old wild type plants and two lines of sensor expressing plants of the T2 generation. Plants were grown on MS medium and analyzed by HPLC. **b**,**c** Confocal images of the fluorescence ratios of a transformed root tip before **b** and 20 min after addition of 10 mM Arg **c**. Scaling bars: 20 μm. **d** Fluorescence ratio increase with time after addition of Arg from confocal imaging. The fluorescence intensity of that section is shown as *inset*. **e** Representative time course of a typical fluorescence ratio using an inverted microscope from an experiment in which Gln and later Arg were added. **f** Similar recording from a plant expressing the Arg-insensitive double mutant sensor ($QBP^{T70A,D157N}$/Citrine/ECFP) with Gln and Arg. The traces in **e** and **f** were corrected for FRET decay due to photobleaching. Glutamine and Arginine were added at 10 mM concentration

attempts, so that continuous long time visualization of individual protoplasts was rather difficult. Continuous monitoring of the fluorescence could only be obtained in a few adhered cells (n=6) after the addition of Arg.

In vivo imaging of Arg uptake in plant roots

The sensors were stably expressed in Arabidopsis plants and studied for Arg-dependent fluorescence changes (Fig. 7). In the plants used, strong ectopic sensor expression in roots and leaves was ensured by the use of the 35S promoter from cauliflower mosaic virus. The strongest fluorescence was generally observed in T1 plants but, in some cases, the fluorescence remained bright in the T2 generation.

HPLC analysis was used to determine whether expression of the sensor constructs affected the total amino acid content in plants. A strong fluorescent line (OBP/citrine/ECFP-1) and a weaker fluorescent line were compared to wild type plants. When grown on standard Murashige-Skoog media, the amino acid arginine was one of the most prominent amino acids in all plants (Fig. 7a). Importantly, the amino acid profile was similar in wild type and sensor expressing plants, suggesting that expression of the sensor only minimally affects the endogenous arginine metabolism and content (Fig. 7a). However, the amount of proline, an amino acid commonly associated with stress responses, differed somewhat between the samples. If this is due to expression of the sensors or to other factors, may need to be verified in future analysis. Both Gln and Arg were taken up and utilized by Arabidopsis roots, as was apparent from growth tests on these amino acids as sole nitrogen source (*data not shown*). In sensor expressing plant lines, a fluorescence ratio increase was observed after the addition of Arg in the root tip (Fig. 7b,c). Without addition of Arg, no increase in the FRET ratio was detected. A representative trace from the time dependent fluorescence ratio change from continuous confocal monitoring of a cross section of the root is shown in Fig. 7d. The fluorescence intensity of that section is shown as inset. It is clearly visible that the fluorescence was excluded from the large vacuoles.

In additional experiments using the inverted microscope, no responses were observed after the addition of Gln to roots (Fig. 7e). In plants expressing the arginine-insensitive double mutant construct $OBP^{T70A,D157N}$/citrine/ECFP, the fluorescence was insensitive to Gln and Arg (Fig. 7f). As this construct contains the same chromophores and responded similarly to the pH, it appears that environmental factors such as pH are unlikely to be responsible for the FRET ratio changes by Arg. A slow fluorescence decrease with time was invariably observed without adding amino acids (*data not shown*) and probably reflects bleaching of the chromophores, primarily of the acceptor chromophore citrine. The specific fluorescence increase with Arg, but not with Gln, suggests specificity of the sensor in plant cells.

Discussion

Construction of a novel fluorescent sensor for Arg

Bacterial periplasmic binding proteins have been widely recognized as highly specific sensor proteins that can couple conformational changes into a change in fluorescent readout [14]. Biosensors covering a large concentration range of substrates have been constructed by mutations in the original sequences. Many of these sensors rely on covalently coupled small fluorophore dyes, which limit their usability in living cells. In contrast, genetically encoded sensors with attached GFP-based chromophores have several advantages, including stable expression in the cells. In addition, such sensors can be targeted to specific cellular compartments using appropriate targeting sequences [8]. However, the environmental sensitivity of the chromophores may itself impose problems on the specificity of the sensors [11]. The yellow fluorescent protein and some of its derivatives have been shown to be sensitive to low pH and high anion concentrations. Secondary effects on the fluorescence have largely been ruled out by using the environmentally insensitive version of YFP, citrine [21]. Within the pH values expected for the cytosol, the FRET ratio of the sensors differed only marginally. By the parallel use of sensors with the same chromophores, but with different amino acid binding receptor domains and different substrate spectrum, environmental effects on the chromophores can be ruled out.

In this study, the QBP protein was used as a reporter element for a genetically encoded FRET-based sensor. The resulting chimeric sensor was highly specific to Arg and Orn, instead of Gln. However, QBP is structurally similar to the Lys/Arg/Orn binding protein LAOBP from *E. coli*. Although both proteins have only 35% amino acid identity, several residues that form hydrogen bonds or ionic interactions with the ligand in the binding pocket are conserved between QBP and the LAOBP. Two residues that have been proposed to confer specificity to Gln in QBP versus Arg/Orn, are the lysine at position 115 and the histidine at position 156 [18]. Both residues are positioned in the same lobe into which citrine was inserted in our chimeric construct. Molecular modeling suggested that the chromophore insertion slightly bent and affected the original structure. The chromophore insertion may therefore explain the unexpected substrate profile of the chimeric sensor. Mutations at residues lysine 115 and histidine 156 may be used in future work to alter the substrate binding

properties of the sensor and may widen its application for sensing other amino acids.

A fluorescent glutamate sensor has recently been reported and has been expressed in the cytosol and on the surface of mammalian cells. This sensor did not change its fluorescence upon glutamate addition when expressed in the cytosol [13]. However, it had a relatively small fluorescence ratio change upon glutamate, which may have concealed small cytosolic glutamate changes. Optimization of the sensors, for example by linker optimization, may lead to better visualization of amino acid changes [25]. The use of different FRET donor/acceptor pairs may also be useful to further magnify the substrate-dependent fluorescence ratio changes in cells in the future [26]. Computational design may be used to widen the substrate range of individual sensors [27].

Fluorescent metabolite sensing in plant cells

The expression of the fluorescent sensors in plant cells showed that such constructs can visualize amino acid uptake into the cytoplasm. Despite the sensors' suitability for in vivo imaging applications in plants, the relatively small ratio change and the sensitivity range still limit the application of the current versions. However, over time many improvements have been made on the Ca-*cameleon* sensors, and these sensors have given ample proof of their usefulness [11]. Fluorescent non-invasive metabolite sensing is especially promising for applications in which other methods are clearly limited. Several differentiated plant tissues, such as the phloem, are relatively inaccessible with current methods. Similarly, the small size and cellular heterogeneity of the young embryo and the seed suggest that metabolite sensors with cellular and sub-cellular resolution may help to unravel metabolite distribution in such structures. It will be interesting to see if the usability of these sensors is expanded by targeting to different compartments and/or by the use of tissue specific promoters. The current constructs were expressed from the 35S cauliflower mosaic virus promoter. In plants expressing these constructs, we observed some variability in the fluorescence intensity. Gene silencing may be involved, and the use of silencing-deficient mutant plants may circumvent this problem [9]. Preliminary results in our laboratory, where fluorescent constructs were expressed using endogenous plant specific promoters, suggest that fluorescence can be observed in subsequent generations.

A direct comparison between the in vivo and in vitro FRET ratios of the sensors is impossible due to the different instrumentation used for the measurements. The illumination devices, recording bandwidth and filters were distinct. The apparent in vitro K_d for Arg may even deviate from the true K_d depending on wavelength and filters chosen [28]. The application of the metabolite sensors in bacteria (Fig. 5) and in plant protoplasts (Fig. 6) suggests that the background fluorescence and possible inner filtering effects impair a direct comparison of the FRET ratios in vitro and in vivo. It is likely that additional sensors that cover a range of intermediate and high affinities are required to provide a firm estimate of cytosolic Arg in plant tissues. The arginine-insensitive double mutant sensor $OBP^{T70A,D157N}$/citrine/ECFP can act as an internal control.

A fluorescent sensor for Arg may be of interest for the analysis of several cellular and biochemical processes, and this is not restricted to plants. Besides acting as a precursor for the synthesis of proteins, Arg plays several additional roles in microbes, plants and animal cells. The biosynthesis of this amino acid is compartmentalized (cytosol, mitochondria and chloroplasts) and Arg is a precursor of urea, polyamines, proline and glutamate [29]. Arg is a substrate of NO production in animals and in plants [30]. The total Arg concentrations in *Arabidopsis* plants grown on soil are in the submillimolar range [31], but in MS-grown plants, Arg is one of the most prominent amino acids (Fig. 7a). Assuming equal distribution in plant tissues, the Arg concentration is in the range of several mM; however, the Arg content analyzed per fresh weight basis does not directly reflect the Arg concentration in the cytoplasm.

The expression of the sensors did not affect the total amount of each amino acid in transgenic plants. In addition, the development and morphology of the sensor-expressing plants was unchanged, suggesting that the Arg binding protein in the cytosol was well buffered and did not limit Arg supply. Arg may vary several-fold in plants and increased approximately 4-fold in tomato as a response to ammonia feeding [32]. Sulphate deprivation raised Arg by a factor of 40× in spinach [33]. Increased Arg was an early response to phosphate deficiency [34]. In contrast to plants, yeast may accumulate Arg up to 430 mM [35] and the accumulated nitrogen may later be released upon starvation. In addition, it has recently been suggested that Arg is the major transferred amino acid in the arbuscular mycorrhizal (AM) symbiosis. These AM fungi form a specific symbiosis with selected plants, but although arginine is the major nitrogen form transported within the fungi, the transferred species to the the plant is less clear [36].

Despite clear limitations, the novel sensors and future improved versions promise to be valuable in the investigation of Arg metabolism and transport across the plant plasma membrane. Transporters that are specific for cationic amino acids have been molecularly identified in plants and are currently being investigated [37]. Genetically encoded Arg sensors that are targeted to various subcellular compartments may be ideal tools to dissect the

complex Arg metabolism that involves cytosol, mitochondria and chloroplasts in plants.

Acknowledgements We thank Petra Neumann (ZMBP, University of Tübingen) for excellent technical help, Bettina Stadelhofer and Harald Stransky for the HPLC analysis, Marek Dynowski (ZMBP, University of Tübingen) for the modeling and display of the structures; and F. de Courcy, B. Neuhäuser and M. Krebs (ZMBP, University of Tübingen) for critically reading the manuscript.

References

1. Coruzzi G, Bush DR (2001) Nitrogen and carbon nutrient and metabolite signaling in plants. Plant Physiol 125:61–64
2. Walch-Liu P, Liu LH, Remans T, Tester M, Forde BG (2006) Evidence that L-glutamate can act as an exogenous signal to modulate root growth and branching in *Arabidopsis thaliana*. Plant Cell Physiol 47:1045–1057
3. Galili G, Hofgen R (2002) Metabolic engineering of amino acids and storage proteins in plants. Metab Eng 4:3–11
4. Goldraij A, Polacco JC (2000) Arginine degradation by arginase in mitochondria of soybean seedling cotyledons. Planta 210:652–658
5. Farre EM, Tiessen A, Roessner U, Geigenberger P, Trethewey RN, Willmitzer L (2001) Analysis of the compartmentation of glycolytic intermediates, nucleotides, sugars, organic acids, amino acids, and sugar alcohols in potato tubers using a nonaqueous fractionation method. Plant Physiol 127:685–700
6. Fernie AR, Trethewey RN, Krotzky AJ, Willmitzer L (2004) Metabolite profiling: from diagnostics to systems biology. Nat Rev Mol Cell Biol 5:763–769
7. Medintz IL, Deschamps JR (2006) Maltose-binding protein: a versatile platform for prototyping biosensing. Curr Opin Biotechnol 17:17–27
8. Fehr M, Okumoto S, Deuschle K, Lager I, Looger LL, Persson J, Kozhukh L, Lalonde S, Frommer WB (2005) Development and use of fluorescent nanosensors for metabolite imaging in living cells. Biochem Soc Trans 33:287–290
9. Deuschle K, Chaudhuri B, Okumoto S, Lager I, Lalonde S, Frommer WB (2006) Rapid metabolism of glucose detected with FRET glucose nanosensors in epidermal cells and intact roots of Arabidopsis RNA-silencing mutants. Plant Cell 18:2314–2325
10. Schroeder JI, Allen GJ, Hugouvieux V, Kwak JM, Waner D (2001) Guard cell signal transduction. Annu Rev Plant Physiol Plant Mol Biol 52:627–658
11. Zhang J, Campbell RE, Ting AY, Tsien RY (2002) Creating new fluorescent probes for cell biology. Nat Rev Mol Cell Biol 3:906–918
12. Fehr M, Frommer WB, Lalonde S (2002) Visualization of maltose uptake in living yeast cells by fluorescent nanosensors. Proc Natl Acad Sci U S A 99:9846–9851
13. Okumoto S, Looger LL, Micheva KD, Reimer RJ, Smith SJ, Frommer WB (2005) Detection of glutamate release from neurons by genetically encoded surface-displayed FRET nanosensors. Proc Natl Acad Sci U S A 102:8740–8745
14. de Lorimier RM, Smith JJ, Dwyer MA, Looger LL, Sali KM, Paavola CD, Rizk SS, Sadigov S, Conrad DW, Loew L, Hellinga HW (2002) Construction of a fluorescent biosensor family. Protein Sci 11:2655–2675
15. Dattelbaum JD, Lakowicz JR (2001) Optical determination of glutamine using a genetically engineered protein. Anal Biochem 291:89–95
16. Weiner JH, Furlong CE, Heppel LA (1971) A binding protein for L-glutamine and its relation to active transport in *E. coli*. Arch Biochem Biophys 142:715–717
17. Hsiao CD, Sun YJ, Rose J, Wang BC (1996) The crystal structure of glutamine-binding protein from *Escherichia coli*. J Mol Biol 262:225–242
18. Sun YJ, Rose J, Wang BC, Hsiao CD (1998) The structure of glutamine-binding protein complexed with glutamine at 1.94 A resolution: comparisons with other amino acid binding proteins. J Mol Biol 278:219–229
19. Hajdukiewicz P, Svab Z, Maliga P (1994) The small, versatile pPZP family of Agrobacterium binary vectors for plant transformation. Plant Mol Biol 25:989–994
20. Mayer M, Dynowski M, Ludewig U (2006) Ammonium ion transport by the AMT/Rh homolog LeAMT1;1. Biochem J 396:431–437
21. Griesbeck O, Baird GS, Campbell RE, Zacharias DA, Tsien RY (2001) Reducing the environmental sensitivity of yellow fluorescent protein. Mechanism and applications. J Biol Chem 276:29188–29194
22. Dixit R, Cyr R, Gilroy S (2006) Using intrinsically fluorescent proteins for plant cell imaging. Plant J 45:599–615
23. Laube B, Schemm R, Betz H (2004) Molecular determinants of ligand discrimination in the glutamate-binding pocket of the NMDA receptor. Neuropharmacology 47:994–1007
24. Burkovski A, Kramer R (2002) Bacterial amino acid transport proteins: occurrence, functions, and significance for biotechnological applications. Appl Microbiol Biotechnol 58:265–274
25. Deuschle K, Okumoto S, Fehr M, Looger LL, Kozhukh L, Frommer WB (2005) Construction and optimization of a family of genetically encoded metabolite sensors by semirational protein engineering. Protein Sci 14:2304–2314
26. Nguyen AW, Daugherty PS (2005) Evolutionary optimization of fluorescent proteins for intracellular FRET. Nat Biotechnol 23:355–360
27. Looger LL, Dwyer MA, Smith JJ, Hellinga HW (2003) Computational design of receptor and sensor proteins with novel functions. Nature 423:185–190
28. Whitaker JE, Haugland RP, Prendergast FG (1991) Spectral and photophysical studies of benzo[c]xanthene dyes: dual emission pH sensors. Anal Biochem 194:330–344
29. Wu G, Morris SM Jr (1998) Arginine metabolism: nitric oxide and beyond. Biochem J 336:1–17
30. Crawford NM (2006) Mechanisms for nitric oxide synthesis in plants. J Exp Bot 57:471-478
31. Pilot G, Stransky H, Bushey DF, Pratelli R, Ludewig U, Wingate VP, Frommer WB (2004) Overexpression of GLUTAMINE DUMPER1 leads to hypersecretion of glutamine from Hydathodes of Arabidopsis leaves. Plant Cell 16:1827–1840
32. Magalhaes JR, Wilcox GE (1984) Growth, free amino acids, and mineral composition of tomato plants in relation to nitrogen form and growing media. J Am Soc Hortic Sci 109:406–411
33. Prosser IM, Purves JV, Saker LR, Clarkson DT (2001) Rapid disruption of nitrogen metabolism and nitrate transport in spinach plants deprived of sulphate. J Exp Bot 52:113–121
34. Rabe E, Lovatt CJ (1986) Increased arginine biosynthesis during phosphorus deficiency a response to the increased ammonia content of leaves. Plant Physiol 81:774–779
35. Kitamoto K, Yoshizawa K, Ohsumi Y, Anraku Y (1988) Dynamic aspects of vacuolar and cytosolic amino acid pools of *Saccharomyces cerevisiae*. J Bacteriol 170:2683–2686
36. Govindarajulu M, Pfeffer PE, Jin H, Abubaker J, Douds DD, Allen JW, Bucking H, Lammers PJ, Shachar-Hill Y (2005) Nitrogen transfer in the arbuscular mycorrhizal symbiosis. Nature 435:819–823
37. Su YH, Frommer WB, Ludewig U (2004) Molecular and functional characterization of a family of amino acid transporters from *Arabidopsis*. Plant Physiol 136:3104–3113